Original Article

Evaluation of the Diagnostic Performance of F18-Fluorodeoxyglucose-Positron Emission Tomography, Dynamic Susceptibility Contrast Perfusion, and Apparent Diffusion Coefficient in Differentiation between Recurrence of a High-grade Glioma and Radiation Necrosis

Sameer Peer, R. Gopinath[1], Jitender Saini[1], Pardeep Kumar[1], Dwarkanath Srinivas[2], Chandana Nagaraj[3]

Department of Radiodiagnosis, AIIMS, Bathinda, Punjab, Departments of [1]Neuro Imaging and Interventional Radiology and [2]Neurosurgery, NIMHANS, [3]Department of Nuclear Medicine, St. Johns National Academy of Health Sciences, Bengaluru, Karnataka, India

Abstract

Background: Differentiation between recurrence of brain tumor and radiation necrosis remains a challenge in current neuro-oncology practice despite recent advances in both radiological and nuclear medicine techniques. **Purpose:** The purpose of this study was to compare the diagnostic performance of dynamic susceptibility contrast (DSC) perfusion magnetic resonance imaging (MRI), apparent diffusion coefficient (ADC) derived from diffusion-weighted imaging, and F18-fluorodeoxyglucose-positron emission tomography (F18-FDG-PET) in the differentiation between the recurrence of a high-grade glioma and radiation necrosis. **Materials and Methods:** Patients with a diagnosis of high-grade glioma (WHO Grades III and IV) who had undergone surgical resection of the tumor followed by radiotherapy with or without chemotherapy were included in the study. DSC perfusion, diffusion-weighted MRI, and PET scan were acquired on a hybrid PET/MRI scanner. For each lesion, early and delayed tumor-to-brain ratio (TBR), early and delayed maximum standardized uptake value (SUV_{max}), normalized ADC ratio, and normalized relative cerebral blood volume (rCBV) ratio were calculated and the pattern of lesional enhancement was noted. The diagnosis was finalized with either histopathological examination or the characteristics on follow-up imaging. The statistical analysis using the receiver operator characteristic curves was done to determine the diagnostic performance of DSC perfusion, 18-F FDG-PET, and ADC in differentiation between tumor recurrence and radiation necrosis. **Results:** Fifty patients were included in the final analysis, 32 of them being men (64%). A cutoff value of early TBR >0.8 (sensitivity of 100% and specificity of 80%), delayed TBR >0.93 (sensitivity of 92.3% and specificity of 80%), early SUV_{max} >10.2 (sensitivity of 76.9% and specificity of 80%), delayed SUV_{max} >13.2 (sensitivity of 61.54% and specificity of 100%), normalized rCBV ratio >1.21 (sensitivity of 100% and specificity of 60%), normalized ADC ratio >1.66 (sensitivity of 38.5% and specificity of 80%), and Grade 3 enhancement (sensitivity of 100% and specificity of 60%) were found to differentiate recurrence from radiation necrosis. Early TBR had the highest accuracy (94.44%), while ADC ratio had the lowest accuracy (50%). A combination of early TBR (cutoff value of 0.8), late TBR (cutoff value of 0.93), and rCBV ratio (cutoff value of 1.21) showed a sensitivity of 100%, specificity of 92.3%, positive predictive value of 88.9%, negative predictive value of 93.7%, and an accuracy of 96.6% in discrimination between radiation necrosis and recurrence of tumor. **Conclusion:** F18-FDG-PET and DSC perfusion can reliably differentiate tumor recurrence from radiation necrosis, with early TBR showing the highest accuracy. ADC demonstrates a low sensitivity, specificity, and accuracy in differentiating radiation necrosis from recurrence. A combination of early TBR, delayed TBR, and rCBV may be more useful in discrimination between radiation necrosis and recurrence of glioma, with this combination showing a better diagnostic performance than individual parameters or any other combination of parameters.

Keywords: *Magnetic resonance imaging, perfusion, positron emission tomography, recurrence, tumor*

Address for correspondence:
Dr. Chandana Nagaraj, Department of Nuclear Medicine, St. Johns National Academy of Health Sciences, Bengaluru, Karnataka, India.
E-mail: chandana.nagaraj@stjohns.in

Received: 18-04-2022
Revised: 20-08-2022
Accepted: 06-09-2022
Published: 08-06-2023

Access this article online

Website: www.ijnm.in

DOI: 10.4103/ijnm.ijnm_73_22

Quick Response Code:

Introduction

The most challenging question in neuro-oncological practice is to differentiate between recurrence of a high-grade glioma and radiation necrosis.[1] This differentiation is vital as the prognosis

How to cite this article: Peer S, Gopinath R, Saini J, Kumar P, Srinivas D, Nagaraj C. Evaluation of the diagnostic performance of F18-fluorodeoxyglucose-positron emission tomography, dynamic susceptibility contrast perfusion, and apparent diffusion coefficient in differentiation between recurrence of a high-grade glioma and radiation necrosis. Indian J Nucl Med 2023;38:115-24.

and further management differs between recurrent tumor and radiation necrosis.[2,3] Many studies have focused on this very research question using various diagnostic techniques. Histopathological diagnosis remains the gold standard in resolving this dilemma of recurrence v/s radiation necrosis is concerned. It may not be a first choice to establish the diagnosis as invasive biopsy has its inherent risks and may further compromise the quality of life of these patients who already have been subjected to aggressive therapies.[4] In the current practice, the advanced magnetic resonance imaging (MRI) techniques including magnetic resonance spectroscopy, diffusion-weighted imaging (DWI), and perfusion-weighted imaging (PWI) along with nuclear medicine imaging techniques such as positron emission tomography (PET) and single-photon emission computed tomography (SPECT) remain the mainstay in the differential diagnosis of tumor recurrence and radiation necrosis.[5-8] With the advent of hybrid imaging modalities such as PET/MRI, we have a unique opportunity to capture the pathophysiology and metabolic characteristics of various brain pathologies in a single session.[9] Dynamic susceptibility contrast (DSC) MRI perfusion is a technique which captures the susceptibility changes occurring in the microvasculature during the first pass of a gadolinium-based contrast agent through the vascular bed.[10] As neoangiogenesis is one of the hallmarks of a high-grade glioma and radiation necrosis is essentially avascular, it is prudent to hypothesize that tumor recurrence should show increased perfusion, as quantified by the relative cerebral blood volume (rCBV), while radiation necrosis should be hypoperfused as compared to normal brain parenchyma.[11] As far as PET is concerned, the recurrent tumor is composed of metabolically active viable cells which show the uptake of the radiopharmaceutical F18-fluorodeoxyglucose (F18-FDG), whereas radiation necrosis may not show any uptake.[12] Diffusion-weighted MRI is expected to show a more restricted diffusion in cases of tumor recurrence as compared with radiation necrosis in view of more cellularity in the former; however, the reported literature is inconsistent in reporting the utility of apparent diffusion coefficient in differentiation of radiation necrosis from recurrence.[4] These techniques are far from being perfect in differentiation of recurrence from radiation necrosis and many false positives and false negatives may be found while interpreting the results of these techniques.[11,12] Although F18-FDG-PET is considered valuable in differentiating radiation necrosis from recurrence, it has now been shown that amino acid PET may provide a more comprehensive clinical information.[12,13]

In this study, we attempted to compare the diagnostic performance of F18-FDG-PET, diffusion-weighted MRI, and DSC MR perfusion in differentiating recurrence in high-grade gliomas from radiation necrosis.

Materials and Methods

A retrospective analysis of patients undergoing hybrid PET/MRI scan from January 2015 to October 2019 was done. Written informed consent was obtained from all the patients before the PET/MRI scan.

Inclusion criteria

All the patients who had undergone treatment for a high-grade glioma (Grade III and IV lesions as defined by the WHO criteria) in the form of surgical resection along with radiotherapy with or without chemotherapy and had been advised a hybrid PET/MRI scan with at least one of the following features were included in the study:

1. New-onset neurological symptoms and/or signs
2. Interval of at least 3 months between chemoradiotherapy and PET/MRI study
3. Follow-up for at least 6 months after PET/MRI study.

All patients who were included in this study had DSC perfusion scan and DWI done in the same session as the PET/MRI scan.

Exclusion criteria

Patients with one or more of the following characteristics were not included in the study:

1. Histopathological diagnosis of the primary tumor not available
2. DSC data not available for analysis
3. DWI not available for analysis
4. No follow-up after hybrid PET/MRI scan.

Classification of the lesion as recurrence or radiation injury

The final diagnosis of a recurrent lesion was obtained by either a surgical biopsy or resection following the PET/MRI study or an interval increase in the size of the enhancing component of the lesion (increase in diameter by more than 25%) with or without antitumor treatment (interval MRI done at least 3 months following PET/MRI study) or appearance of new enhancing lesion at the site of the primary lesion on follow-up MRI.

The diagnosis of radiation injury was made if there was either a reduction in the size of the lesion or stabilization of the contrast-enhancing component of the lesion on interval MRI done at least 6 months after PET/MRI study.

Protocol for positron emission tomography scan

PET data were acquired using hybrid PET/MRI Biograph mMR scanner (Siemens Healthcare, Erlangen, Germany). The patients rested in a quiet and warm dark room for 15 min before FDG administration and during the uptake period. For PET acquisition, an i.v. injection of F18-FDG (3–5 mCi) was administered. Patients were asked to remain fasting for at least 6 h before FDG injection. In

all the cases, the blood glucose was measured at arrival at the center for molecular imaging, NIMHANS, and FDG was injected only if the blood glucose level was below 120 mg/dl.

The static PET data were acquired for 15 min; the matrix size was 344 mm × 344 mm. PET emission data were reconstructed with ordered subset expectation maximization algorithm (21 subsets, 5 iterations) and postfiltered with a three-dimensional (3D) isotropic Gaussian of 2 mm at Full width half maximum (FWHM), resulting in a final spatial resolution of approximately 2 mm along each direction. Attenuation correction was performed using MR-based attenuation maps derived from an ultrashort TE sequence.

Protocol for magnetic resonance imaging scan

MRI scan for all the patients was performed on a 3T simultaneous PET/MRI Biograph mMR scanner (Siemens Healthineers, Erlangen, Germany).

The following MRI sequences were acquired:

i. Precontrast scan included axial and sagittal T1-weighted spin echo (TR/TE – 550/15 ms), axial T2-weighted turbo spin echo (TR/TE – 5500/91 ms), 3D FLAIR (TR/TE/TI – 5000/385/1800, flip angle 120°), DWI with b values of 0 and 1000 s/mm^2, (TR/TE – 4400/70 ms; number of sections-27), and susceptibility weighted imaging with TR/TE – 26/20 ms
ii. DSC perfusion MRI using gradient echo-planar imaging (TR/TE – 2050/30 ms, flip angle – 90°, slice thickness – 4 mm, and field of view – 230 mm × 230 mm). A series of images were taken immediately before, during, and after intravenous injection of a bolus of 10 ml of gadodiamide (Omniscan, GE Healthcare, Chicago, Illinois) at a flow rate of 3–4 ml/sec followed by a saline flush of 10 ml at the rate of 3–4 ml/s using a dual-syringe mechanical pressure injector through a 18G or 20G intravenous cannula
iii. Postcontrast T1W MPRAGE sequence (TR/TE – 2200/2.3 ms, flip angle –8°, slice thickness – 1 mm, and field of view –250 mm × 250 mm) was acquired in sagittal plane following the DSC perfusion MRI in all the cases. The images were then reconstructed in axial and coronal planes on the workstation.

Analysis of positron emission tomography data

The PET data were analyzed in the syngo.via workstation (Siemens Healthineers, Erlangen, Germany). The fused PET/MR images were visually assessed for optimal quality. The maximum standardized uptake value (SUV_{max}) of the lesion and the contralateral normal-appearing cerebral cortex were determined using 3D region of interest (ROI) measurements, as shown in Figure 1. The tumor-to-brain ratio (TBR) was calculated for all the patients as a ratio between the SUV_{max} of the tumor and the SUV_{max} of the contralateral cerebral cortex.

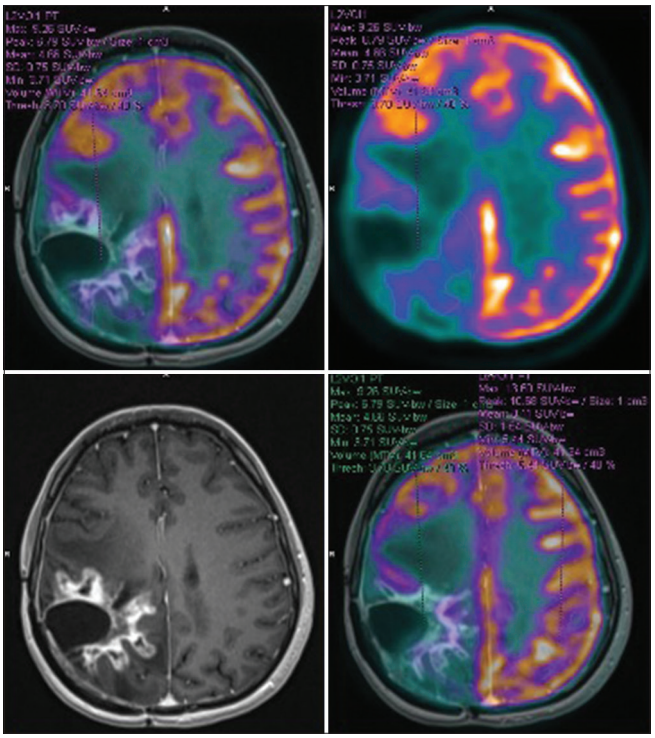

Figure 1: Method for calculation of TBR. TBR is calculated as the ratio of SUV_{max} of the lesion and the SUV_{max} of the normal-appearing cerebral parenchyma, TBR: Tumor-to-brain ratio, SUV_{max}: Maximum standardized uptake value

Early and delayed TBR and early and delayed SUV_{max} were recorded. The average delay between injection of the radiotracer and early image acquisition was 45 min (range: 35 min to 90 min) and the average interval between early and delayed image acquisition was 90 min (range: 60 min to 120 min).

Analysis of dynamic susceptibility contrast perfusion magnetic resonance imaging

DSC perfusion data were analyzed using the Philips IntelliSpace Portal 12.0 (Koninklijke Philips NV, Amsterdam, The Netherlands). Voxel-wise signal-to-time curves were inspected visually for assessment of optimal quality of perfusion data. Leakage correction was used for quantitative analysis of the DSC perfusion data, as depicted in Figure 2. Using postcontrast 3D magnetization-prepared rapid gradient echo (MPRAGE) as an underlay, the corrected rCBV was obtained by drawing an elliptical ROI with an area between 10 mm^2 and 20 mm^2 within the enhancing component of the lesion. A control mirror ROI was drawn in the contralateral cerebral parenchyma to determine the corrected rCBV in that location. Areas corresponding to hemorrhage, vessels, and cystic components were avoided while drawing the ROIs. A normalized rCBV ratio was then calculated by the software as the ratio between the corrected rCBV of the lesion and the corrected rCBV of the contralateral cerebral parenchyma.

Analysis of diffusion-weighted imaging and apparent diffusion coefficient ratio

The apparent diffusion coefficient (ADC) ratio was calculated using the Philips IntelliSpace Portal 12.0 (Koninklijke Philips NV, Amsterdam, The Netherlands). For determination of the ROI, PET images were taken as a guide and an ROI with an area between 10 mm^2 and 20 mm^2 was drawn within the area of uptake on PET and a mirror ROI was drawn within the contralateral normal-appearing brain parenchyma [Figure 3]. The ADC ratio was then calculated as the ratio between the ADC value of the lesion and the contralateral normal-appearing brain parenchyma.

Assessment of the contrast enhancement of the lesion

Postcontrast 3D MPRAGE sequence was used for a visual assessment of the degree of enhancement of the lesion. Using an ordinal grading scale, mild enhancement was given a Grade 1, moderate enhancement was given a Grade 2, and avid enhancement was given a Grade 3, as shown in Figure 4.

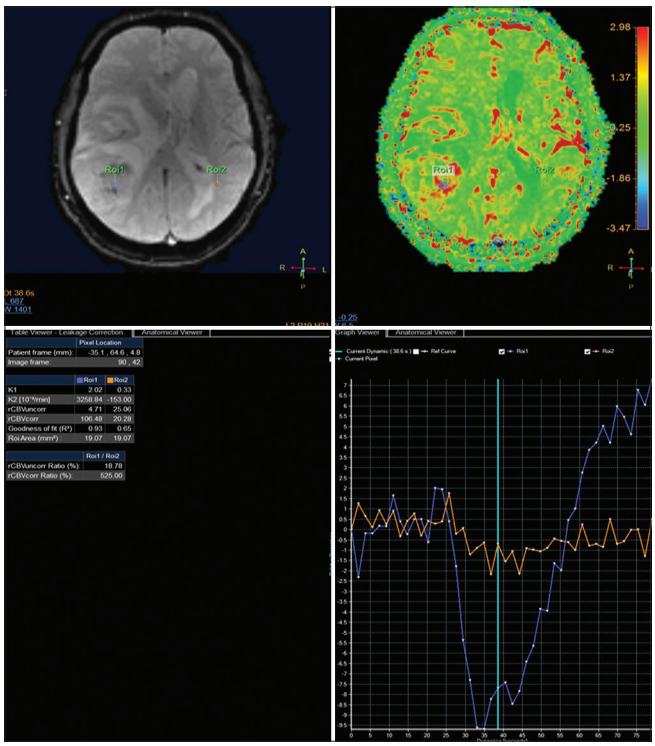

Figure 2: Method used for calculation of normalized rCBV ratios on Philips IntelliSpace Portal 6.0. ROI 1 is drawn within the enhancing component of the lesion as seen on the fused perfusion color map and postcontrast T1W MPRAGE images. ROI 2 is a mirror ROI with the same area as that of ROI 1 and is drawn on the contralateral normal-appearing cerebral parenchyma. The software uses leakage correction to derive the corrected rCBV values and the ratio of corrected rCBV values between ROI 1 and ROI 2. An overshoot of the signal intensity-time curve is noted which indicates effects of contrast leakage and T1 relaxation, rCBV: Relative cerebral blood volume, MPRAGE: Magnetization prepared rapid gradient echo, ROI: Region of interest

Statistical analysis

Statistical analysis was done using MedCalc for Windows (MedCalc Software, Mariakerke, Belgium). All the continuous variables were represented as mean and standard deviation. Mann–Whitney U-test was used to determine the differences in normalized rCBV ratios, ADC ratios, the early and delayed TBR, and the early and delayed SUV_{max} between recurrent lesions and radiation injury. Receiver operator characteristic (ROC) analysis was done for normalized rCBV ratios, ADC ratios, early and delayed SUV_{max}, early and delayed TBR, and the grade of enhancement to determine the area under the curve (AUC) for each of these variables. Youden's J statistic was used to determine the cutoff values for each of the variables to differentiate between recurrent lesion and radiation injury. P <0.05 was chosen as the criteria for statistical significance for all the statistical tests.

Results

Fifty patients were included in the final analysis, 32 of them being men (64%). The average age of the patients was 46 ± 13.8 years (range, 10–64 years). The average time interval between the initial treatment and PET/MRI scan was 19.2 months. Glioblastoma was the most common primary tumor (n = 28, 56%) diagnosed on the initial histopathology. Anaplastic oligodendroglioma (n = 10, 20%), anaplastic oligoastrocytoma (n = 4, 8%), anaplastic ependymoma (n = 3, 6%), and anaplastic astrocytoma (n = 4, 8%) were the other histopathological types of primary tumors diagnosed among the patients. In one case, further classification could not be done on histopathology and it was labeled as anaplastic glioma without further classification. Following PET/MRI study, the final diagnosis was established by surgical resection/biopsy followed by histopathological examination in 22 cases (44%). In the remaining 28 cases (56%), the diagnosis was established on follow-up imaging as per the criteria described earlier. Thirty-six patients (72%) were diagnosed with recurrence and 14 patients (28%) were diagnosed as having radiation injury. Out of the 36 patients with a final diagnosis of recurrence, histopathological confirmation of the diagnosis was possible in 20 cases. In the remaining 16 cases, the diagnosis of recurrence was

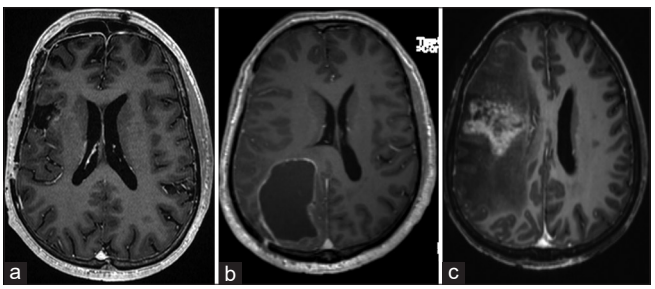

Figure 3: Grading of contrast enhancement on postcontrast T1W MPRAGE images. Grade 1 is shown in (a), Grade 2 in (b), and Grade 3 in (c), MPRAGE: Magnetization prepared rapid gradient echo

based on follow-up imaging criteria. In all the 14 patients with a diagnosis of radiation injury, the final diagnosis was made on the basis of follow-up imaging criteria.

Fifty lesions were analyzed for contrast enhancement, early and delayed TBR, early and delayed SUV_{max} on fused PET/MR images, normalized ADC ratios derived from DWI, and normalized rCBV ratios derived from DSC perfusion. All the lesions showed enhancement on postcontrast T1W MPRAGE sequence. Forty-one lesions (82%) showed Grade 3 enhancement. Grade 2 enhancement was noted in five lesions and Grade 1 enhancement was seen in four lesions. The ROC analysis of the various variables is summarized in Figure 4 and Table 1. The early and delayed TBR, early and delayed SUV_{max}, normalized ADC ratio, and normalized rCBV ratio were found to be higher among the recurrent lesions as compared to the radiation injury, as represented in Table 2, Figures 5 and 6. A cutoff value of 1.21 for normalized rCBV ratio was found to yield a sensitivity of 100%, a specificity of 60%, and an accuracy of 88.9% for the differentiation between radiation necrosis and recurrence. Among the FDG-PET metrics, a cutoff value of 0.8 for early TBR had a sensitivity of 100% and specificity of 80% for differentiating recurrence from radiation necrosis with an accuracy of 94.4%, which was found to be the highest among all the metrics analyzed in this study. A Grade 3 enhancement had a sensitivity of 100% and a specificity of 60% in making a differentiation between recurrence and radiation necrosis with an accuracy

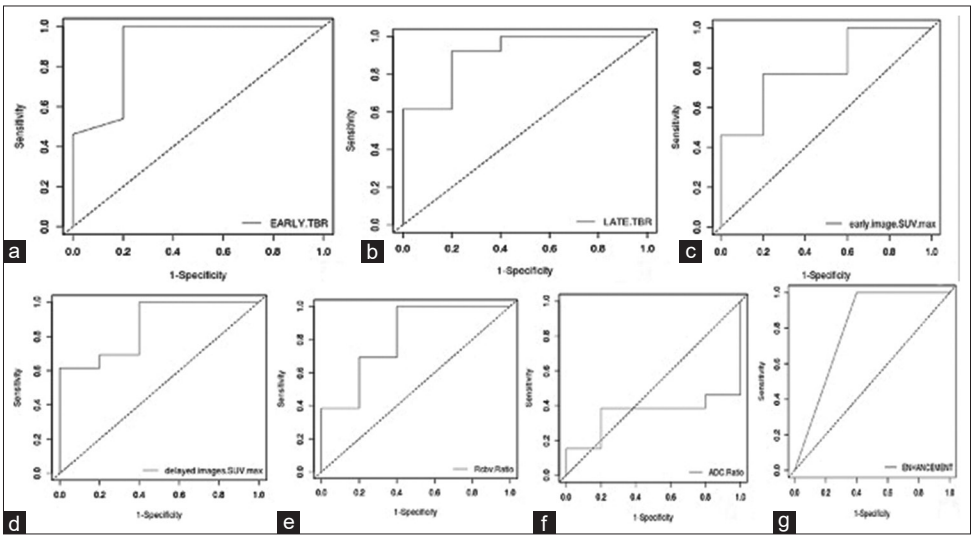

Figure 4: ROC curves for early TBR (a), Delayed TBR (b), Early SUV_{max} (c), Delayed SUV_{max} (d), Normalized rCBV ratio (e), Normalized ADC ratio (f) and Contrast enhancement (g). The highest AUC is noted for delayed TBR (0.097). The lowest AUC is noted for normalized ADC ratio (0.353), ROC: Receiver operator characteristic, TBR: Tumor-to-brain ratio, SUV_{max}: Maximum standardized uptake value, rCBV: Relative cerebral blood volume, ADC: Apparent diffusion coefficient, AUC: Area under the curve

Table 1: Summary of receiver-operator curve analysis

	95% CI							
	Early TBR	**Delayed TBR**	**Early SUV_{max}**	**Delayed SUV_{max}**	**Normalized rCBV ratio**	**Enhancement**	**Normalized ADC ratio**	**Combination (early TBR, delayed TBR, rCBV)**
Area under curve	0.90 (0.69–1.1)	0.907 (0.74–1.07)	0.80 (0.56–1.03)	0.86 (0.66–1.05)	0.815 (0.61–0.95)	0.80 (0.55–1.04)	0.353 (0.09–0.61)	0.91 (.72–1.09)
Cutoff value	0.8	0.93	10.2	13.2	1.21	Grade 3	1.66	(0.8,0.93,1.21)
Sensitivity (%)	100 (75.3–100)	92.3 (64.6–97.8)	76.9 (42.4–87.9)	61.54 (39.2–81.6)	100 (74.7–100)	100 (74.7–100)	38.5 (25.8–54.7)	100 (74.7–100)
Specificity (%)	80 (72.3–99.5)	80 (72.3–99.5)	80 (72.3–99.5)	100 (65.1–100)	60 (58.2–76.3)	60 (58.2–76.3)	80 (67.5–93.6)	92.3 (75.3–99.7)
Positive predictive value (%)	92.8 (68.2–95.9)	92.3 (67.5–98.4)	90.9 (63.2–96.2)	100 (60.5–100)	86.6 (68.5–93.6)	86.6 (68.5–93.6)	83.3 (71.5–92.3)	88.9 (72.4–97.3)
Negative predictive value (%)	100 (79.1–100)	80 (47.8–93.8)	57.1 (32.1–75.3)	50 (26.3–61.7)	100 (73.7–100)	100 (73.7–100)	33.3 (19.7–51.2)	93.7 (73.7–98.5)
Accuracy (%)	94.4 (85.7–100)	88.9 (70.2–97.9)	77.8 (53.8–89.9)	72.22 (45.3–82.4)	88.9 (62.6–95.5)	88.9 (62.6–95.5)	50 (32.6–61.5)	96.6 (74.3–99.6)

TBR: Tumor-to-brain ratio, rCBV: Relative cerebral blood volume, CI: Confidence interval, ADC: Apparent diffusion coefficient, SUV_{max}: Maximum standardized uptake value

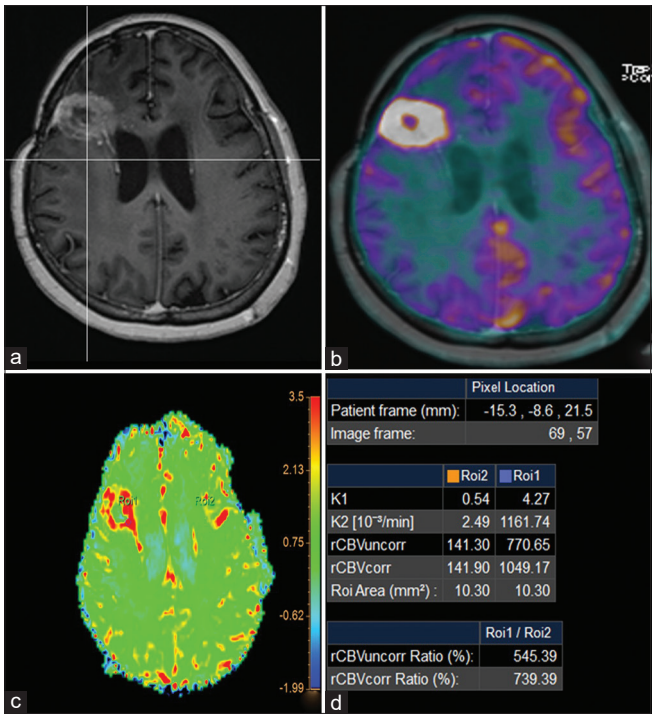

Figure 5: A 47-year-old woman who had undergone surgical resection of right frontal glioblastoma followed by chemoradiation, presented with headache and seizures 21 months after the initial treatment. A well-defined lesion is seen in the right frontal lobe with Grade 3 contrast enhancement on axial postcontrast T1W MPRAGE (a), Fused 18F-FDG-PET/MRI image (b) shows avid uptake of the radiopharmaceutical with TBR of 2.82. DSC perfusion color map (c) and quantitative analysis of the perfusion parameters using leakage correction in Philips IntelliSpace Portal 6.0 (d) show elevated corrected rCBV within the lesion with normalized rCBV ratio of 7.93. The diagnosis of recurrence of glioblastoma was confirmed after surgical biopsy and histopathology, MPRAGE: Magnetization prepared rapid gradient echo, 18F-FDG-PET: F18-Fluorodeoxyglucose-positron emission tomography, MRI: Magnetic resonance imaging, TBR: Tumor-to-brain ratio, DSC: Dynamic susceptibility contrast, rCBV: Relative cerebral blood volume

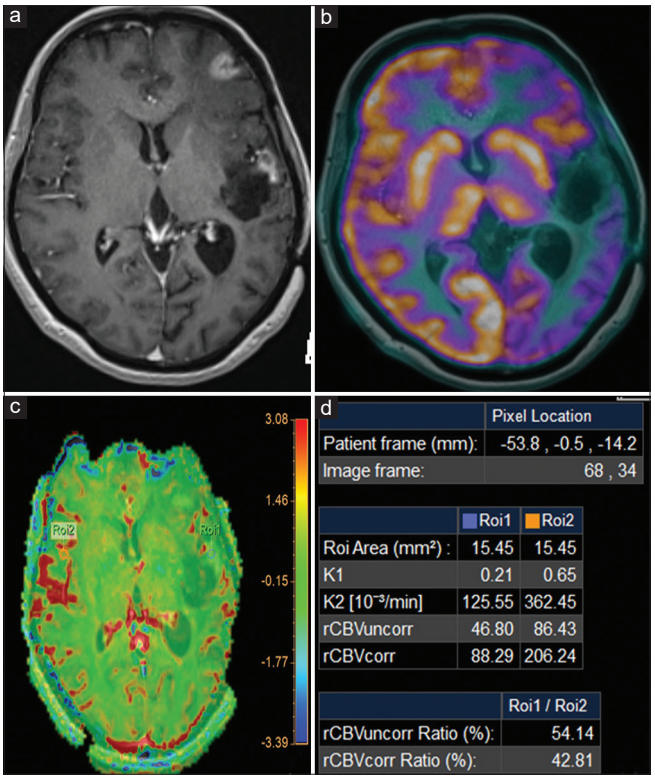

Figure 6: 44-year-old female was treated for anaplastic oligo-astrocytoma with surgical resection of the tumour followed by chemoradiation. She presented 28 months later with headache and vomiting. Axial post-contrast T1W MPRAGE image (a) shows patchy areas of post-contrast enhancement adjacent to the post-operative cavity. There was no obvious uptake in the lesion on 18F-FDG PET on visual assessment (b) and the TBR was 0.85. DSC perfusion color maps and (c) quantitative data from the analysis in Philips intellispace portal 6.0 shows no evidence of elevated perfusion within the lesion with (d) normalized rCBV value of 0.42. Follow-up MRI at 6 months and 12 months after PET/MRI scan (not shown) showed gradual reduction in the enhancing component of the lesion and a final diagnosis of radiation necrosis was made

Table 2: Results of the Mann–Whitney *U*-test

Parameter	Mean		*P*
	Recurrence	Radiation necrosis	
Early TBR	1.7±0.88	0.72±0.60	0.012
Delayed TBR	1.9±0.97	0.85±0.30	0.01
Early SUV_{max}	14.08±6.13	7.91±3.26	0.06
Delayed SUV_{max}	16.81±5.31	7.96±2.77	0.02
Normalized rCBV ratio	4.44±8.57	1.93±1.35	0.04
Normalized ADC ratio	1.51±0.64	1.62±0.18	0.37
Enhancement (Grade 3) (%)	36 (100)	5 (36)	0.009

TBR: Tumor-to-brain ratio, rCBV: Relative cerebral blood volume, ADC: Apparent diffusion coefficient, SUV_{max}: Maximum standardized uptake value

of 88.9%. Normalized ADC ratio with a cutoff of 1.66 had a sensitivity of 38.5% and a specificity of 80% for differentiating radiation necrosis from recurrence with an accuracy of 50%, which was the lowest among all the other metrics. The area under ROC curve was the highest for late TBR (0.907) and the lowest for normalized ADC ratio (0.35). Performance analysis after combining various metrics revealed that a combination of early TBR (cutoff value of 0.8), late TBR (cutoff value of 0.93), and rCBV ratio (cutoff value of 1.21) showed a sensitivity of 100%, specificity of 92.3%, positive predictive value of 88.9%, negative predictive value (NPV) of 93.7% and an accuracy of 96.6% in discrimination between radiation necrosis and recurrence of tumor. This performance measured was better than individual performances of each of the parameters as well as any other combination of parameters.

Discussion

High-grade glioma is a term which encompasses WHO Grade III and Grade IV gliomas. Among the high-grade gliomas, glioblastomas are considered the most aggressive and account for approximately 15%–20% of all primary intracranial tumors.[14] Recurrence is common in high-grade gliomas, and it has been shown that the mean time since initial treatment to recurrence is approximately 32–36 weeks in glioblastoma.[15] Recurrence occurs due to continuous neoplastic activity within a margin of 2–3 cm from the primary neoplasm.[15] The standard of

care management of high-grade gliomas includes surgery, radiotherapy, and chemotherapy.[16] With increasing use of multimodality approaches to glioma management, the risk of radiation necrosis posttreatment of gliomas has increased.[1] Radiation necrosis is considered a late complication of brain irradiation and usually occurs months to years after the radiation exposure.[1] Among the various risk factors for development of radiation necrosis in gliomas, total radiation dose, fraction size, and chemotherapy are thought to be important.[17]

Radiation necrosis may have an appearance on conventional imaging which may be indistinguishable from tumor recurrence.[18,19] Although various patterns of contrast enhancement, such as "soap" bubble appearance and "Swiss cheese" appearance, have been described for radiation necrosis, these are not specific and may be seen in recurrent tumors as well.[18,19] In a study by Mullins *et al*. evaluating the conventional MRI features for distinguishing radiation necrosis from recurrence in gliomas, involvement of the corpus callosum along with various combinations of other findings, such as multiple enhancing foci, crossing of midline, and subependymal spread, were suggestive of progression of glioma.[20]

The performance of DSC MR perfusion has been evaluated in various studies. Sugahara *et al*. evaluated the value of DSC perfusion in differentiating tumor recurrence from nonneoplastic enhancing lesions in 20 patients. They included various types of neoplasms in their study including astrocytoma (Grades II and IV), ganglioglioma, germinoma, and primitive neuroectodermal tumor. They found that a normalized rCBV ratio of more than 2.6 was suggestive of recurrence whereas that of <0.6 was suggestive of nonneoplastic enhancing tissue. They further concluded that between normalized rCBV ratio of 2.6 and 0.6, ^{201}Tl-SPECT could help in differentiating the two.[21] In a retrospective study on 57 patients with glioblastoma, Barajas *et al*. found that the mean, maximum, and minimum relative peak height and rCBV values were significantly higher in recurrence of glioblastoma as compared to the radiation necrosis. They also showed that the mean, maximum, and minimum percentage signal recovery was significantly lower in recurrent glioblastoma as compared to radiation necrosis.[6] In a prospective study on 42 tissue specimens in 13 patients with high-grade gliomas, Hu *et al*. reported a threshold value of 0.71 for rCBV to differentiate between recurrence and radiation necrosis with a sensitivity of 91.7% and specificity of 100%.[22] Solimana *et al*. reported a threshold value of 1.8 for relative peak height and 1.22 for rCBV to differentiate recurrent glioma from radiation necrosis on DSC perfusion on the basis of a study on 20 patients with Grade II to Grade IV gliomas treated with surgery and radiotherapy with or without chemotherapy.[23] There is a lot of variation in the literature regarding the thresholds of perfusion metrics for differentiating radiation necrosis and recurrence. In our study, we found that a threshold of normalized rCBV ratio of 1.21 could differentiate recurrence from radiation necrosis with a sensitivity of 100% and specificity of 60%. The variation may be accounted for by the differences in the patient characteristics, the histopathological types of tumors, the imaging protocol used, the method of deriving the perfusion parameters, etc., which can vary from institution to institution and from one scanner to another.

F18-FDG-PET has been used as a tool for differentiating radiation necrosis and recurrence for many years. Di Chiro *et al*. reported a 100% sensitivity and specificity of 18F-FDG-PET in differentiating radiation necrosis from recurrence.[24] They had a histopathological diagnosis in all their cases. Another study by Valk *et al*. showed a sensitivity and specificity of 88% and 81%, respectively, of 18F-FDG for the diagnosis of radiation necrosis versus recurrence.[25] However, there are few studies which have demonstrated a lower sensitivity and specificity of 18F-FDG-PET because of the physiological tracer uptake of the brain which is the major disadvantage. For instance, Ricci *et al*., in their study on 31 patients with histopathological confirmation of diagnosis, found a sensitivity of 73% and specificity of 56% for differentiating radiation necrosis from recurrence.[26] Chao *et al*. reported an overall sensitivity of 75% and a specificity of 80%. They used MRI and PET co-registration in their study and found that for brain metastasis, there was an improvement of sensitivity from 65% (PET alone) to 86% (PET with MRI co-registration).[27] An inflammatory response in radiation necrosis may be one of the reasons for false-positive results when evaluating 18F-FDG in such cases.[28] Recently, amino acid PET has been used to differentiate radiation necrosis from recurrence. Hotta *et al*. used radiomics approach in 11C-methionine PET for differentiation of recurrence from radiation necrosis. They found that radiomics and tumor-to-normal ratio had a sensitivity of 90.1% and 60.6% and specificity of 93.9% and 72.7%, respectively.[29]

There have been only a few studies in the literature which have compared two or more modalities simultaneously for differentiation of radiation necrosis and recurrence. Kumar *et al*. compared DSC perfusion and 18F-FDG-PET in 28 cases (23 primary brain tumors and 5 metastatic lesions). They found that DSC perfusion had an accuracy of 94.5% as compared to 85.1% of 18F-FDG-PET for differential diagnosis of recurrence and radiation necrosis.[30] Tomura *et al*. studied 18 metastatic brain lesions in 15 patients who had undergone Gamma Knife radiosurgery. They compared 11C-methionine-PET, 18F-FDG-PET, MR permeability, and ADC for differentiating recurrence from radiation necrosis. They concluded that 11-C-methionine PET may be superior to MR-permeability scan and ADC in this regard.[31] A recent study by Qiao *et al*. compared 11C-methionine-PET/CT and DSC perfusion MRI for the purpose of differentiating radiation necrosis from recurrence in 42 patients (33 – recurrence and 9 – radiation injury).

11C-methionine PET/CT showed a sensitivity of 0.909 and specificity of 0.556, while DSC perfusion showed sensitivity and specificity of 0.667 and 0.778, respectively. The optimal cutoffs for tumor-to-background SUV_{max} and mean rCBV were 1.85 and 1.83, respectively. They concluded that both 11C-methionine PET/CT and PWI were equally accurate in differentiation of recurrence from radiation injury in high-grade gliomas.[32] Another study by Hojjati *et al*. compared FDG-PET/MRI, FDG-PET/CT, and DSC perfusion MRI in differentiating radiation necrosis from recurrence in glioblastoma. For PET/MRI, a relative mean ≥1.31 yielded an AUC of 0.94 with a 100% sensitivity and NPV. For DSC perfusion, CBV_{max} ≥3.32 yielded AUC of 0.94 with sensitivity and NPV of 100%. Joint model of relative mean (PET/MRI) and CBV (DSC perfusion) resulted in AUC of 1.0. They concluded that a combination of DSC perfusion with PET/MRI parameters had the best diagnostic value in differentiation of radiation necrosis from recurrence in glioblastoma.[33]

Diffusion-weighted MRI is sensitive to the Brownian motion of protons inside a particular voxel. ADC, derived from DWI, is a measure of diffusion of protons within a voxel (measured in units mm^2/s).[34] A high cellularity confers restriction of anisotropic motion of water molecules, thereby lowering the ADC.[34] Intuitively, tumor recurrence should depict a lower ADC than radiation necrosis. However, the literature is inconsistent when it comes to reporting the ADC values in recurrence and radiation necrosis. Sundgren *et al*. reported a higher ADC value in recurrence as compared to radiation-induced changes.[35] Other studies by Hien *et al*.,[36] Xu *et al*.,[37] and Zeng *et al*.[38] reported a lower ADC value in recurrence. In a recent study by Zakhari *et al*.,[39] central diffusion restriction within a lesion was found to be indicative of radiation necrosis rather than recurrence. An interplay of vasogenic edema, necrosis, extracellular space enlargement, and gliosis could confound the otherwise seemingly straightforward and intuitive interpretation of ADC in differentiating radiation necrosis from recurrence.

In our study, we simultaneously compared TBR (early and delayed) and SUV_{max} (early and delayed) derived from 18F-FDG, normalized ADC ratio derived from DWI, and normalized rCBV ratios derived from DSC perfusion. The rationale behind evaluating early and delayed TBR and SUV_{max} is the improved sensitivity and specificity of detection of malignant lesions and their differentiation from benign lesions, as demonstrated by Kubota *et al*.,[40] Basu *et al*.,[41] and Suga *et al*.[42] Indeed, we found early TBR to be the most accurate in differentiating radiation necrosis from recurrence. rCBV ratios had a fairly good sensitivity, specificity, and accuracy in this regard as well. Contrast enhancement, graded visually, also had a comparable diagnostic performance with DSC perfusion, both having a high sensitivity (100%) but a low specificity (60%). The other metrics derived from F18-FDG-PET had a lower accuracy when compared with early TBR, DSC perfusion, and enhancement. The normalized ADC ratio had a very low sensitivity (38.5%) and accuracy (50%) in differentiating radiation necrosis from recurrence. This low diagnostic performance of ADC could be explained by the factors discussed earlier, such as vasogenic edema, necrotic component, and expansion of extracellular space and presence of gliotic scar tissue postradiotherapy which may complicate the ADC calculation. Our results indicate that it may be more useful to combine early TBR, delayed TBR, and rCBV ratio, in order to differentiate radiation necrosis from recurrence of glioma, since the accuracy, sensitivity, specificity, positive predictive value, and NPV of a combination of these parameters yielded a better diagnostic performance than individual parameters.

Various challenges are faced once PET/MRI is used as a diagnostic modality in evaluation of this problem of differentiating radiation necrosis from recurrence. Attenuation correction in PET/MRI is a problem since MRI is based on proton density and tissue relaxivity characteristics and does not provide direct information regarding electron density in contrast to PET/CT.[43] Various techniques have been attempted to resolve the issue of attenuation correction in PET/MRI such as pseudo-CT generation, zero TE sequence, atlas-based approaches, and Dixon-based approaches and new methods based on machine learning algorithms are being developed.[43] As far as DSC perfusion is concerned, contrast leakage from intravascular to extravascular compartment is one of the pitfalls in analysis of perfusion data.[10] Due to contrast leakage, T1 effects may overcome the DSC perfusion effects and may underestimate the rCBV.[44] Blood–brain barrier disruption is a characteristic feature of high-grade gliomas, and T1 effects may be predominant while computing rCBV using DSC perfusion.[44,45] In this situation, leakage correction algorithm may improve the accuracy of quantification of the rCBV values using DSC perfusion.[10,46] Blood–brain barrier disruption is also a feature of radiation necrosis.[1,19] We used leakage correction algorithm for analysis of DSC perfusion data as contrast leakage is a concern in both high-grade gliomas and radiation necrosis.

We acknowledge that a relative sample size may be considered a limitation of this study. Another limitation could be the nonavailability of histopathological confirmation of the diagnosis in all the cases.

Conclusion

Eighteen- FDG-PET and DSC perfusion can reliably differentiate tumor recurrence from radiation necrosis, with early TBR showing the highest accuracy for the differentiation at a cutoff value of 0.8. ADC demonstrates a low sensitivity, specificity, and accuracy in differentiating radiation necrosis from recurrence. A combination of early TBR, delayed TBR, and rCBV is the most useful approach

with best diagnostic performance in differentiating radiation necrosis from recurrence of glioma.

Declaration of patient consent

The authors certify that they have obtained all appropriate patient consent forms. In the form the patient (s) has/have given his/her/their consent for his/her/their images and other clinical information to be reported in the journal. The patients understand that their names and initial s will not be published and due efforts will be made to conceal their identity, but anonymity cannot be guaranteed

Acknowledgment

We would like to thank Dr. Sandhya Mangalore, Dr. Arpana Arbind, Mr. Dinesh Kumar, and Mr. Raman Kumar Joshi for contributing in data acquisition and interpretation.

Financial support and sponsorship

This study did not receive any funding from any governmental or nongovernmental organization.

Conflicts of interest

There are no conflicts of interest.

References

1. Chao ST, Ahluwalia MS, Barnett GH, Stevens GH, Murphy ES, Stockham AL, *et al.* Challenges with the diagnosis and treatment of cerebral radiation necrosis. Int J Radiat Oncol Biol Phys 2013;87:449-57.
2. Loganadane G, Dhermain F, Louvel G, Kauv P, Deutsch E, Le Péchoux C, *et al.* Brain radiation necrosis: Current management with a focus on non-small cell lung cancer patients. Front Oncol 2018;8:336.
3. Mallick S, Benson R, Hakim A, Rath GK. Management of glioblastoma after recurrence: A changing paradigm. J Egypt Natl Canc Inst 2016;28:199-210.
4. Verma N, Cowperthwaite MC, Burnett MG, Markey MK. Differentiating tumor recurrence from treatment necrosis: A review of neuro-oncologic imaging strategies. Neuro Oncol 2013;15:515-34.
5. Sanghvi DA. Recent advances in imaging of brain tumors. Indian J Cancer 2009;46:82-7.
6. Barajas RF Jr., Chang JS, Segal MR, Parsa AT, McDermott MW, Berger MS, *et al.* Differentiation of recurrent glioblastoma multiforme from radiation necrosis after external beam radiation therapy with dynamic susceptibility-weighted contrast-enhanced perfusion MR imaging. Radiology 2009;253:486-96.
7. Minamimoto R, Saginoya T, Kondo C, Tomura N, Ito K, Matsuo Y, *et al.* Differentiation of brain tumor recurrence from post-radiotherapy necrosis with 11C-Methionine PET: Visual assessment versus quantitative assessment. PLoS One 2015;10:e0132515.
8. Chuang MT, Liu YS, Tsai YS, Chen YC, Wang CK. Differentiating radiation-induced necrosis from recurrent brain tumor using MR perfusion and spectroscopy: A meta-analysis. PLoS One 2016;11:e0141438.
9. Jadvar H, Colletti PM. Competitive advantage of PET/MRI. Eur J Radiol 2014;83:84-94.
10. Leu K, Boxerman JL, Cloughesy TF, Lai A, Nghiemphu PL, Liau LM, *et al.* Improved leakage correction for single-echo dynamic susceptibility contrast perfusion MRI estimates of relative cerebral blood volume in high-grade gliomas by accounting for bidirectional contrast agent exchange. AJNR Am J Neuroradiol 2016;37:1440-6.
11. Muto M, Frauenfelder G, Senese R, Zeccolini F, Schena E, Giurazza F, *et al.* Dynamic susceptibility contrast (DSC) perfusion MRI in differential diagnosis between radionecrosis and neoangiogenesis in cerebral metastases using rCBV, rCBF and K2. Radiol Med 2018;123:545-52.
12. Hustinx R, Pourdehnad M, Kaschten B, Alavi A. PET imaging for differentiating recurrent brain tumor from radiation necrosis. Radiol Clin North Am 2005;43:35-47.
13. Galldiks N, Lohmann P, Albert NL, Tonn JC, Langen KJ. Current status of PET imaging in neuro-oncology. Neurooncol Adv 2019;1:vdz010.
14. Hanif F, Muzaffar K, Perveen K, Malhi SM, Simjee SU. Glioblastoma Multiforme: A Review of its Epidemiology and Pathogenesis through Clinical Presentation and Treatment. Asian Pac J Cancer Prev 2017;18:3-9. doi: 10.22034/APJCP.2017.18.1.3.
15. Ammirati M, Galicich JH, Arbit E, Liao Y. Reoperation in the treatment of recurrent intracranial malignant gliomas. Neurosurgery 1987;21:607-14.
16. Khan MN, Sharma AM, Pitz M, Loewen SK, Quon H, Poulin A, *et al.* High-grade glioma management and response assessment-recent advances and current challenges. Curr Oncol 2016;23:e383-91.
17. Ruben JD, Dally M, Bailey M, Smith R, McLean CA, Fedele P. Cerebral radiation necrosis: Incidence, outcomes, and risk factors with emphasis on radiation parameters and chemotherapy. Int J Radiat Oncol Biol Phys 2006;65:499-508.
18. Shah R, Vattoth S, Jacob R, Manzil FF, O'Malley JP, Borghei P, *et al.* Radiation necrosis in the brain: Imaging features and differentiation from tumor recurrence. Radiographics 2012;32:1343-59.
19. Fatterpekar GM, Galheigo D, Narayana A, Johnson G, Knopp E. Treatment-related change versus tumor recurrence in High-grade gliomas: A diagnostic conundrum – Use of dynamic susceptibility contrast-enhanced (DSC) perfusion MRI. AJR Am J Roentgenol 2012;198:19-26.
20. Mullins ME, Barest GD, Schaefer PW, Hochberg FH, Gonzalez RG, Lev MH. Radiation necrosis versus glioma recurrence: Conventional MR imaging clues to diagnosis. AJNR Am J Neuroradiol 2005;26:1967-72.
21. Sugahara T, Korogi Y, Tomiguchi S, Shigematsu Y, Ikushima I, Kira T, *et al.* Posttherapeutic intraaxial brain tumor: The value of perfusion-sensitive contrast-enhanced MR imaging for differentiating tumor recurrence from nonneoplastic contrast-enhancing tissue. AJNR Am J Neuroradiol 2000;21:901-9.
22. Hu LS, Baxter LC, Smith KA, Feuerstein BG, Karis JP, Eschbacher JM, *et al.* Relative cerebral blood volume values to differentiate High-grade glioma recurrence from posttreatment radiation effect: Direct correlation between image-guided tissue histopathology and localized dynamic susceptibility-weighted contrast-enhanced perfusion MR imaging measurements. AJNR Am J Neuroradiol 2009;30:552-8.
23. Solimana HM, El Beheirya AA, Abdel-Kerima AA, Farhoud AH, Reda MI. Recurrent brain tumor versus radiation necrosis; can dynamic susceptibility contrast (DSC) perfusion magnetic resonance imaging differentiate? Egypt J Radiol Nucl Med 2018;49:719-26.
24. Di Chiro G, Oldfield E, Wright DC, De Michele D, Katz DA,

Patronas NJ, *et al.* Cerebral necrosis after radiotherapy and/or intraarterial chemotherapy for brain tumors: PET and neuropathologic studies. AJR Am J Roentgenol 1988;150:189-97.
25. Valk PE, Budinger TF, Levin VA, Silver P, Gutin PH, Doyle WK. PET of malignant cerebral tumors after interstitial brachytherapy. Demonstration of metabolic activity and correlation with clinical outcome. J Neurosurg 1988;69:830-8.
26. Ricci PE, Karis JP, Heiserman JE, Fram EK, Bice AN, Drayer BP. Differentiating recurrent tumor from radiation necrosis: Time for re-evaluation of positron emission tomography? AJNR Am J Neuroradiol 1998;19:407-13.
27. Chao ST, Suh JH, Raja S, Lee SY, Barnett G. The sensitivity and specificity of FDG PET in distinguishing recurrent brain tumor from radionecrosis in patients treated with stereotactic radiosurgery. Int J Cancer 2001;96:191-7.
28. Fischman AJ, Thornton AF, Frosch MP, Swearinger B, Gonzalez RG, Alpert NM. FDG hypermetabolism associated with inflammatory necrotic changes following radiation of meningioma. J Nucl Med 1997;38:1027-9.
29. Hotta M, Minamimoto R, Miwa K. 11C-methionine-PET for differentiating recurrent brain tumor from radiation necrosis: Radiomics approach with random forest classifier. Sci Rep 2019;9:15666.
30. Kumar Y, Gupta N, Mangla M, Hooda K, Mangla R. Comparison between MR perfusion and 18F-FDG PET in differentiating tumor recurrence from nonneoplastic contrast-enhancing tissue. Asian Pac J Cancer Prev 2017;18:759-63.
31. Tomura N, Kokubun M, Saginoya T, Mizuno Y, Kikuchi Y. Differentiation between treatment-induced necrosis and recurrent tumors in patients with metastatic brain tumors: Comparison among ^{11}C-Methionine-PET, FDG-PET, MR permeability imaging, and MRI-ADC-preliminary results. AJNR Am J Neuroradiol 2017;38:1520-7.
32. Qiao Z, Zhao X, Wang K, Zhang Y, Fan D, Yu T, *et al.* Utility of dynamic susceptibility contrast perfusion-weighted MR imaging and ^{11}C-Methionine PET/CT for differentiation of tumor recurrence from radiation injury in patients with High-grade gliomas. AJNR Am J Neuroradiol 2019;40:253-9.
33. Hojjati M, Badve C, Garg V, Tatsuoka C, Rogers L, Sloan A, *et al.* Role of FDG-PET/MRI, FDG-PET/CT, and dynamic susceptibility contrast perfusion MRI in differentiating radiation necrosis from tumor recurrence in Glioblastomas. J Neuroimaging 2018;28:118-25.
34. Baliyan V, Das CJ, Sharma R, Gupta AK. Diffusion weighted imaging: Technique and applications. World J Radiol 2016;8:785-98.
35. Sundgren PC, Fan X, Weybright P, Welsh RC, Carlos RC, Petrou M, *et al.* Differentiation of recurrent brain tumor versus radiation injury using diffusion tensor imaging in patients with new contrast-enhancing lesions. Magn Reson Imaging 2006;24:1131-42.
36. Hein PA, Eskey CJ, Dunn JF, Hug EB. Diffusion-weighted imaging in the follow-up of treated high-grade gliomas: Tumor recurrence versus radiation injury. AJNR Am J Neuroradiol 2004;25:201-9.
37. Xu JL, Li YL, Lian JM, Dou SW, Yan FS, Wu H, *et al.* Distinction between postoperative recurrent glioma and radiation injury using MR diffusion tensor imaging. Neuroradiology 2010;52:1193-9.
38. Zeng QS, Li CF, Liu H, Zhen JH, Feng DC. Distinction between recurrent glioma and radiation injury using magnetic resonance spectroscopy in combination with diffusion-weighted imaging. Int J Radiat Oncol Biol Phys 2007;68:151-8.
39. Zakhari N, Taccone MS, Torres C, Chakraborty S, Sinclair J, Woulfe J, *et al.* Diagnostic accuracy of centrally restricted diffusion in the differentiation of treatment-related necrosis from tumor recurrence in High-grade gliomas. AJNR Am J Neuroradiol 2018;39:260-4.
40. Kubota K, Itoh M, Ozaki K, Ono S, Tashiro M, Yamaguchi K, *et al.* Advantage of delayed whole-body FDG-PET imaging for tumour detection. Eur J Nucl Med 2001;28:696-703.
41. Basu S, Kung J, Houseni M, Zhuang H, Tidmarsh GF, Alavi A. Temporal profile of fluorodeoxyglucose uptake in malignant lesions and normal organs over extended time periods in patients with lung carcinoma: Implications for its utilization in assessing malignant lesions. Q J Nucl Med Mol Imaging 2009;53:9-19.
42. Suga K, Kawakami Y, Hiyama A, Sugi K, Okabe K, Matsumoto T, *et al.* Dual-time point 18F-FDG PET/CT scan for differentiation between 18F-FDG-avid non-small cell lung cancer and benign lesions. Ann Nucl Med 2009;23:427-35.
43. Chen Y, An H. Attenuation correction of PET/MR imaging. Magn Reson Imaging Clin N Am 2017;25:245-55.
44. Nakajima S, Okada T, Yamamoto A, Kanagaki M, Fushimi Y, Okada T, *et al.* Differentiation between primary central nervous system lymphoma and glioblastoma: A comparative study of parameters derived from dynamic susceptibility contrast-enhanced perfusion-weighted MRI. Clin Radiol 2015;70:1393-9.
45. Toh CH, Wei KC, Chang CN, Ng SH, Wong HF. Differentiation of primary central nervous system lymphomas and glioblastomas: Comparisons of diagnostic performance of dynamic susceptibility contrast-enhanced perfusion MR imaging without and with contrast-leakage correction. AJNR Am J Neuroradiol 2013;34:1145-9.
46. Kim YS, Choi SH, Yoo RE, Kang KM, Yun TJ, Kim JH, *et al.* Leakage correction improves prognosis prediction of dynamic susceptibility contrast perfusion MRI in primary central nervous system lymphoma. Sci Rep 2018;8:456.